

# Robotic Blood Vessel Mechanism to Realize Active Self-Healing Function for Inflatable Actuators\*

Kenjiro TADAKUMA, Shohei INOMATA, Masahiro WATANABE, Issei ONDA, Eri TAKANE,  
Yuta YAMAZAKI, Fumiya SHIGA, Masanori KAMEOKA, MD Nahin Islam SHIBLEE,  
Hidemitsu FURUKAWA and Satoshi TADOKORO

**Abstract**— This paper presents a novel approach to improving the self-repair capabilities of soft robots by introducing a self-contained robotic blood vessel mechanism. Aimed at addressing the physical weakness of soft robots from sharp objects, the proposed system is inspired by biological healing processes, utilizing water-absorbent materials to seal damage actively. The study validates the effectiveness of this mechanism through experimental evaluation, showing that the self-healing function is enhanced as the channel area within the wound cross-section is increased. Future directions for research include the optimization of material placement and the adaptation of the system for repeated injuries, paving the way for more resilient inflatable soft robots with active self-healing functions.

## I. INTRODUCTION

In recent years, soft robots have been actively researched and developed in the field of robotics. Owing to their flexibility, soft robots can be used in various applications that require shape adaptability, affinity for the human body, shock absorption, and large deformability. However, many soft robots are damaged by contact with sharp objects because of their flexible body structure, resulting in a loss of functionality, such as mobility and deformability. Consequently, research and development of materials with self-healing functions has been conducted in the field of materials, particularly polymeric materials [1]-[4]. However, these self-healing materials require an energy supply from external sources, such as ultraviolet irradiation and heating, as well as maintaining adhesion to the damaged part during self-healing. In addition, in environments with many impurities, such as sand and dust, the adhesion of impurities to the cross-sectional surfaces of the self-healing material reduces their strength. Further, restoration of the functionality following the creation of a hole by focusing on the self-repair mechanism is another active research topic. For example, a method for closing a wound by utilizing the expansion of water-absorbing polymers has been proposed [5]. However, most conventional methods encounter difficulties in self-repairing damage above a certain size. Thus, this study proposed a soft robotic vascular mechanism that enables rapid and active self-repairs in soft robots. The results of an evaluation experiment on the self-repair capability of a soft robotic vascular mechanism in a balloon structure wherein expansion pressure was applied to a plate-like base material, have been discussed.

\*Research supported by MEXT Grant-in-Aid for Scientific Research on Innovative Areas, Science of Soft Robot Interdisciplinary integration of mechatronics, material science, and bio-computing, Grant Number 18H05471.

Kenjiro Tadakuma is with the Tough Cyberphysical AI Research Center and Graduate School of Information Sciences, Tohoku University, Japan (corresponding author to provide email: tadakuma@rm.is.tohoku.ac.jp).

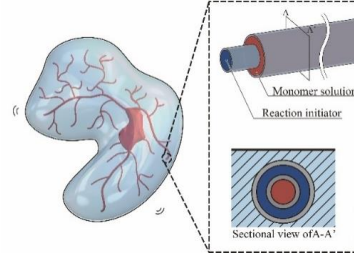


Figure 1. Basic concept of the Robotic Blood Vessels

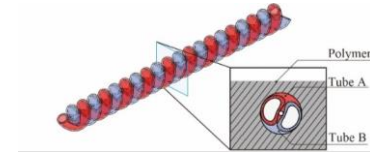


Figure 2. Blood Vessels Mechanism with Twisted Configuration

## II. BASIC PRINCIPLE

Fig. 1 illustrates the concept of the developed soft robot blood vessel mechanism. This mechanism comprises blood vessels stretched around a soft robot with a flexible body. When a soft robot is damaged, liquid oozes from the wound and hardens to become a part of the body. This facilitates active repairing by itself. Moreover, this self-repair function is expected to be possible even under various environmental conditions owing to the mechanism of hardening by incorporating impurities, even when they are introduced into the cross-sectional area.

Although vapors in open air and ultraviolet light are possible curing methods for liquids, this study adopted a two-component mixing method as a curing method that is not affected by external factors. Considering the good accelerating property of the mixing of the two liquids, the spiral shape shown in Fig. 2 is considered effective.

Fig. 3 shows an expansion-and-contraction actuator as a typical example of a soft robot with a robotic vascular mechanism. When a balloon mechanism sustains a penetrating wound, air leaks from the penetrating portion, resulting in a loss of functionality. Via the application of the soft robotic vascular mechanism proposed in this study, we attempted to actively repair the wound and restore functionality by causing fluid to ooze out from the damaged area (Fig. 4).

Shohei Inomata, Issei Onda, Eri Takane, and Satoshi Tadokoro are with the Graduate School of Information Sciences, Tohoku University, Japan.

Masahiro Watanabe is with the Tough Cyberphysical AI Research Center, Tohoku University, Japan.

Yuta Yamazaki, Fumiya Shiga, Masanori Kameoka, MD Nahin Islam Shiblee, and Hidemitsu Furukawa are with the Graduate School of Science and Engineering, Yamagata University, Japan.

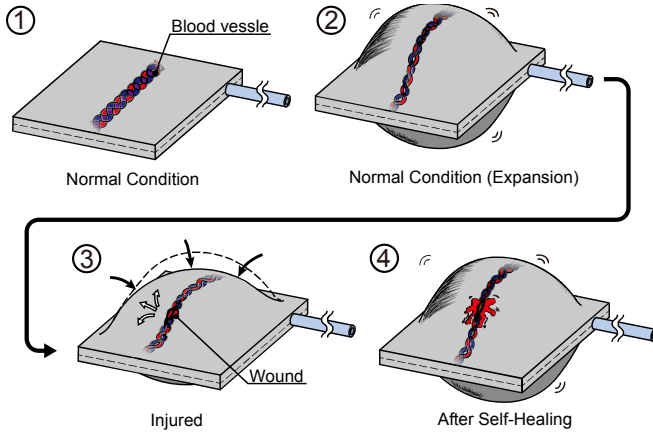


Figure 3. Self-healing by robotic blood vessel mechanism.

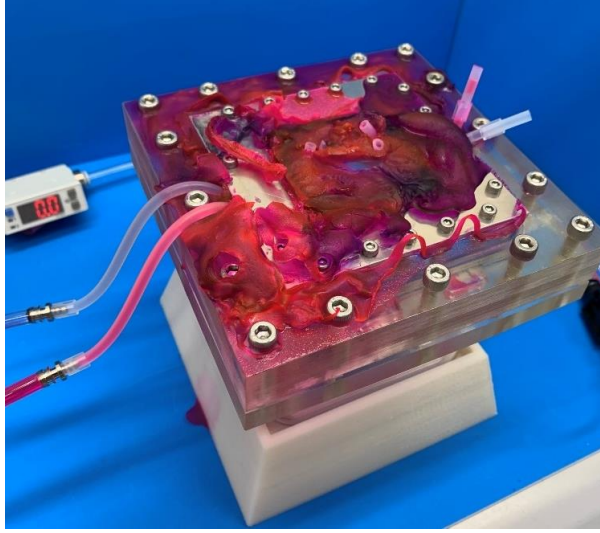


Figure 4. Photo of the wound after self-healing.

### III. ACTUAL EQUIPMENT EMBODIMENT

#### A. Comparative Experiments on Vascular Structure

As a preparatory experiment for experiments using a robotic vascular system with a helix twist structure, an experiment was conducted to confirm whether the mixing of two liquids was possible in a helix twist structure. Fig. 5 shows a model of the robotic vascular mechanism used in the experiment. The specifications are the same as those listed in Table 1. First, red and blue water was injected into the vascular mechanism to increase visibility. Subsequently, a 15-mm-deep and 50-mm-wide incision was made to visually examine the appearance of the oozing water. The same experiment was conducted using two parallel tubes for comparison. Fig. 6 and 7 show the experimental results for the helix-twist and parallel structures, respectively. In case of a parallel incision to the axial direction of the vessel, only one liquid appeared. In contrast, two liquids appeared and mixed in the spiral-twist structure. This was because only one of the two pipes in the parallel structure was damaged. Thus, the helix-twist structure, which has a three-dimensional structure, was advantageous for mixing at the size and depth of the incision in this experiment.

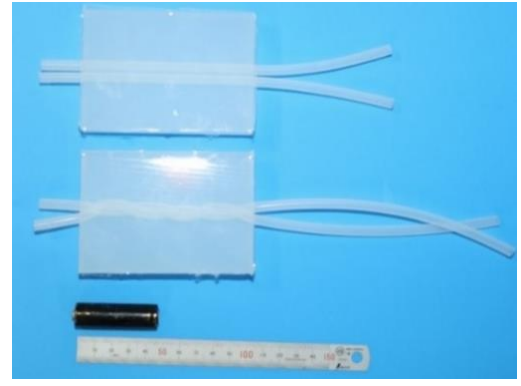


Figure 5. Straight Type and Twisted Type of the Blood Vessel Mechanism

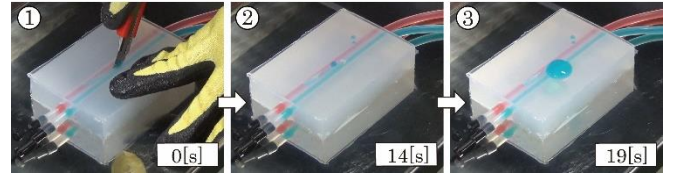


Figure 6. Experiment of mixing of two liquids when scratched in the axial direction (Straight Version)

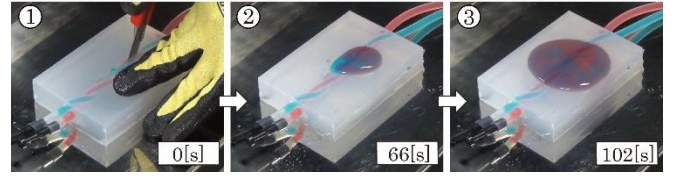


Figure 7. Experiment of mixing of two liquids when scratched in the axial direction (Twisted Version)

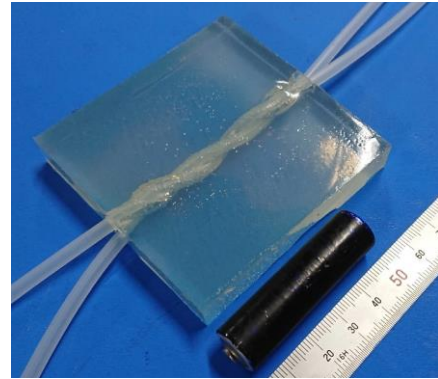


Figure 8. Prototype of embodied soft robotic vascular mechanism

Based on the results of the above basic experiments, Fig. 8 shows an actual prototype soft robotic vascular mechanism with two pairs of spiral tube structures. Table 1 lists the prototype specifications. Considering the difficulty and cost of fabrication, the prototype was fabricated using inter-crosslinked network gel (ICN gel)[6] as the base material and silicone rubber as the tubing material. For the vascular structure, a helix-twist structure was adopted to facilitate the mixing of the two liquids, even for longitudinally penetrating wounds. The helix pitch of the tubing was set at 25 mm to ensure stable construction of the helix without collapsing the tubing.



TABLE I. SPECIFICATIONS OF PROTOTYPE MACHINE

<b>welding base metal</b>	material	ICN Gel
	range (e.g. of voice)	75[mm] (in.)
	length	75[mm] (in.)
	thickness	12[mm].
<b>tube</b>	material	silicone rubber
	the way (of proper conduct, etc.)	Outer diameter 4[mm] Inner diameter 2[mm]
	helix pitch	25[mm].

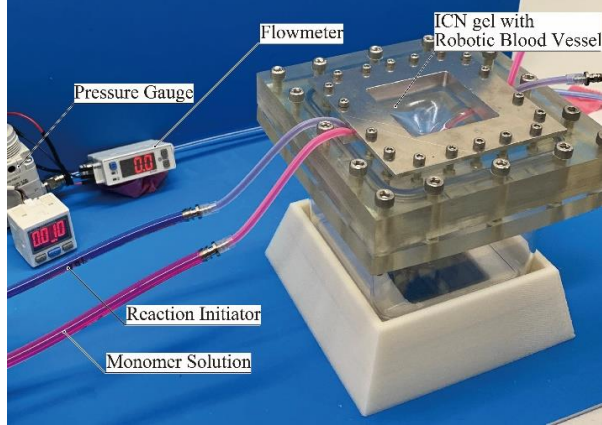


Figure 9. Appearance of experimental apparatus

## IV. EXPERIMENTS ON BASIC EQUIPMENT

## A. Outline of the experiment

Experiments were conducted to evaluate the ability of robotic blood vessels to self-heal under hollow and pressurized inflated conditions, such as in a balloon structure.

Fig. 9 shows the appearance of the experimental apparatus. In this experiment, a prototype machine equipped with a robotic vascular mechanism was attached to the top of a sealed container, and the inside of the container was pressurized to 10 kPa while cutting the membrane. A 10-mm-wide scalpel was used to make an incision by vertically stabilizing the membrane.

The tubes were filled with two liquids: a monomer solution of fine particle-prepared double network gel (P-DN gel) [7] and a radical reaction initiator. To improve visibility during the experiment, pigments were added to the two solutions. The monomer solution was colored red, and the radical reactant was colored blue.

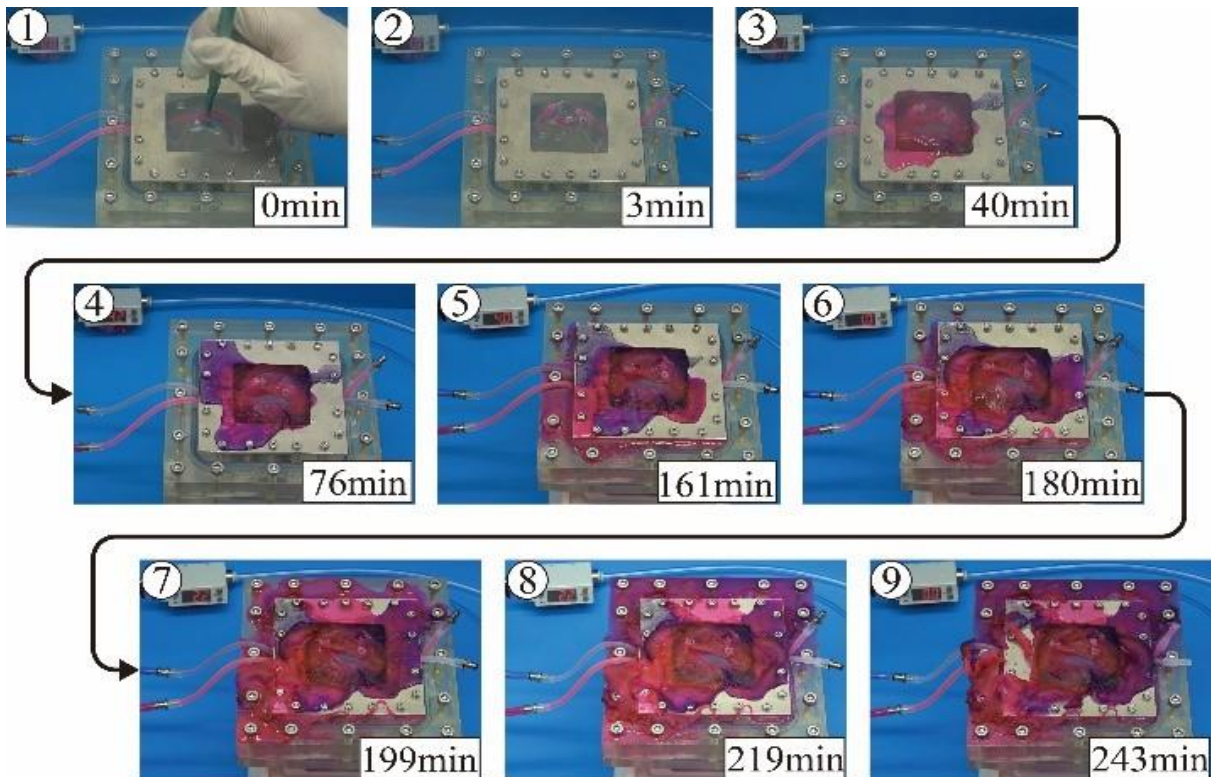


Figure 10. Active self-repair by robotic vascular mechanism

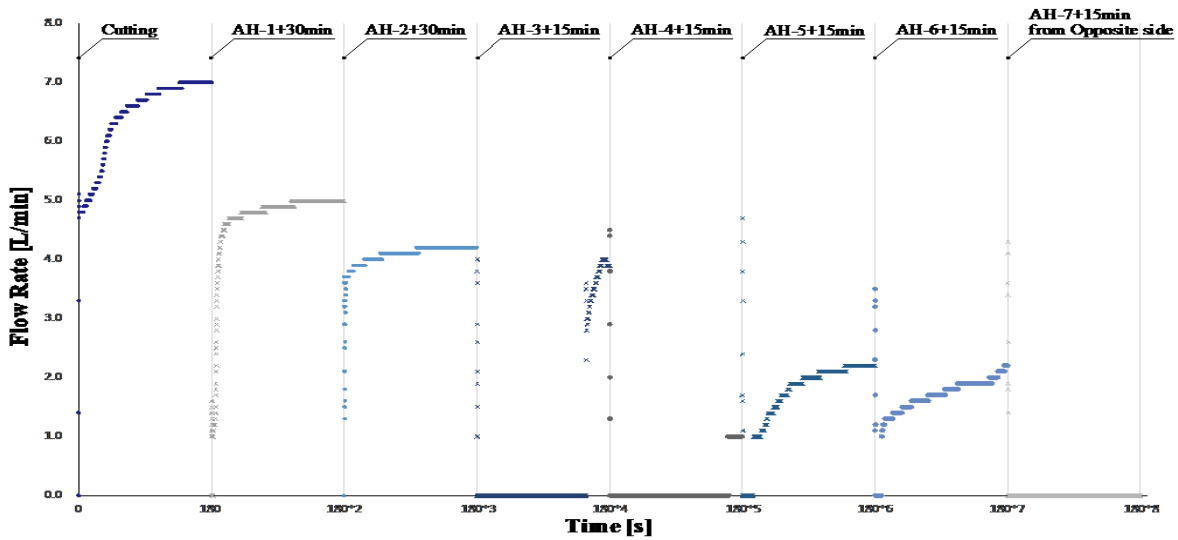


Figure 11. Time variation of the amount of air leakage from the wound during the number of active self-repair cycles.



Figure 12. Enlarged view of the wound area after active self-repair

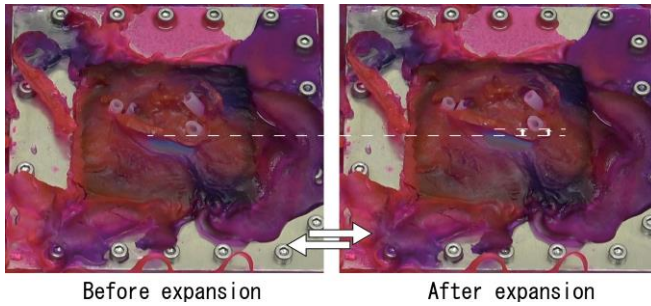


Figure 13. Expansion operation after active repair

### B. Experimental results

Fig. 10 shows the changes in appearance during the experiments. Fig. 11 shows the change in the flow rate for each injection frequency. The horizontal axis shows the passage of time under pressure, and the vertical axis shows the flow rate. Fig. 12 and Fig. 13 shows the enlarged view of the wound area.

The flow rate increased with time in each case; however, this was attributed to the expansion of the wound caused by pressurization.

From the first to the fourth cycle, the flow rate of the leaked air decreased with each cycle. In contrast, the flow rate increased in the fifth and sixth cycles compared with that in the fourth cycle. This was because the gel material did not flow

properly into the wound area. This resulted in air leakage and the wound was not sealed. The seventh injection of gel material in the reverse direction was considered to have closed the wound.

### C. Considerations

In the prototype model fabricated in this study, the tube was pulled out owing to poor adhesion between the ICN gel, base material, silicone rubber, and tubing material. In addition, the use of off-the-shelf silicone rubber tubing caused the wound to expand because of the restoring force in the direction of unraveling the helix in the wounded area. Moreover, as shown in Figure 14, the cross-section of the tube was sometimes oriented toward the inside of the sealed container. In this case, the gel material did not flow into the damaged area, and flowed only into the inside of the container; therefore, self-repair did not occur.

We considered that an effective solution would be to place the blood vessels in a vascular tube with added tension; when a rupture occurs, the tube can pop outward only by exploiting the tension.

### V. EXPERIMENT ON ACTUAL EQUIPMENT WITH WATER-SUPPLY FABRIC SURFACE

Figure 15 shows the appearance of the actual prototype of the soft robotic vascular mechanism. Table 2 summarizes the specifications of the prototype. The plate-shaped prototype

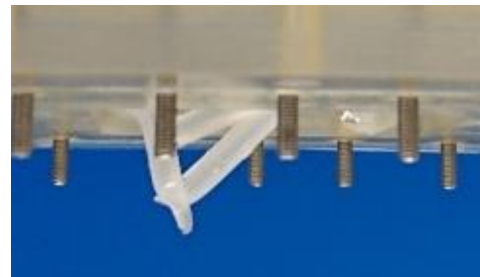


Figure 14. Tube cross section facing inward during infeed Example of not flowing into the wound area due to

was a balloon mechanism, as shown in Fig. 3, with only one side of the balloon removed. The spiral vessel structure mounted on the prototype was made of twisted silicone rubber tubing with a circular cross-section, and the outside of the spiral was coated with silicone rubber to reduce the restorative force of the tubing.

For the liquid flowing through the tube, a monomer solution of the P-DN gel and a radical reaction initiator were used, and the two liquids were mixed for approximately 30 s to prepare the gel.

In addition, the robotic vascular mechanism was positioned as active self-repair from the perspective of utilizing the material that causes the injury and the channels and fluids that allow the material to repair itself, to enable repair in a shorter time. During the construction of an artificial pressure ulcer, soft materials become hard.

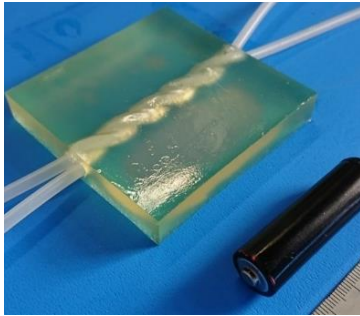


Figure 15. Prototype model of the blood vessel mechanism with coated twisted configuration.

TABLE II. SPECIFICATIONS OF THE TEST PIECE

<b>welding base metal</b>	material	P-DN gel [8].
	width	75 mm
	length	75 mm
	thickness	12 mm
<b>tube</b>	material	silicone rubber
	the way (of proper conduct, etc.)	Outer diameter 4 mm Inner diameter 2 mm
	helix pitch	25 mm
	Coating Thickness	0.5 mm

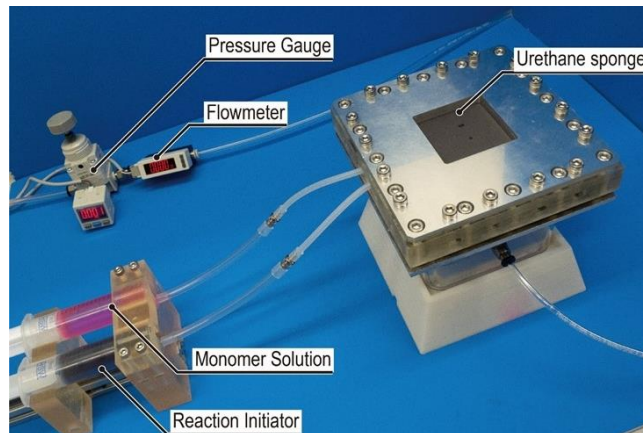


Figure 16. Experimental equipment for air leakage test.

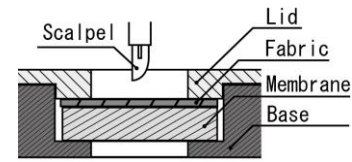


Figure 17. Cross section of test piece fixing part.

#### A. Experiments to evaluate water-absorbing surfaces

When the prototype device is used alone, the high fluidity of the liquid flowing through the pipe may cause the liquid material to flow to a location other than the wound site. We attempted to solve this problem by placing a water-absorbing material on the surface of the membrane to retain the liquid material near the wound.

Fig. 16 shows an overview of the experimental apparatus. Fig. 17 shows the cross section of the membrane and fixed section of the water-absorbent material. Pressure regulated by a pressure gauge and precision regulator was supplied to the experimental apparatus, and a flow meter measured the flow rate of the compressed air. In the event of an air leak, the flowmeter measured the amount of leakage and thus confirmed the presence of an air leak. In other words, the flow rate was measured when there was a penetration wound in the membrane. When the hole was closed by self-repair, the flow rate was lost.

Three types of absorbent materials were prepared for comparison: Jersey fabric, urethane sponge, and gauze. With these materials in place, a pressure of 10 kPa was applied to create a wound. Using a scalpel, scratches were made perpendicular to the axial direction of the helix such that the length of the wound was 15 mm. After wounding, the pressure was released and the liquid material was poured into it. Ten min after pouring, the pressure was applied again to check for air leakage.

Fig. 18 shows the experimental results. Air leakage occurred under all conditions, although the amount of leakage varied immediately after the wound was created. After self-repairing by pouring, air leakage was eliminated under all four conditions, indicating that the wound was sealed. After repeating the expansion and contraction operations assumed for the balloon structure for 10 times, air leakage reappeared only when no water-absorbing material was used. Thus, the water-absorbent surface contributed to the improvement in the self-repair capability.

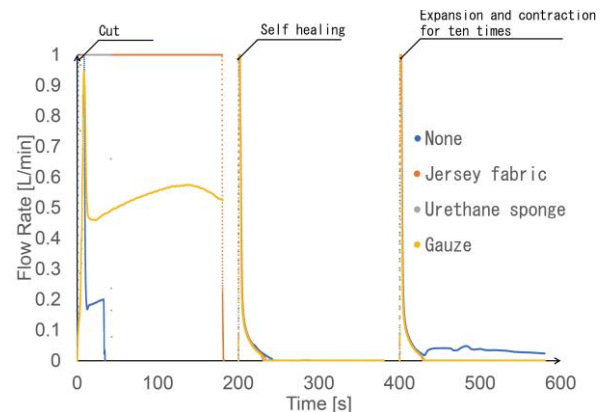


Figure 18. Comparison of liquid absorption surfaces.



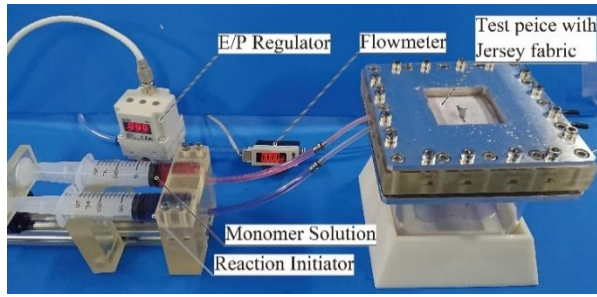


Figure 19. Experimental equipment of Pressure test.

### B. Quantitative evaluation of self-healing capacity

In the previous section, the possibility that water-absorbent surfaces can improve self-healing capability was confirmed. Therefore, in this section, experiments were conducted to quantitatively evaluate the self-healing ability of the material-transported vascular mechanism with jersey fabric, the most stretchable water-absorbing material, placed on the surface.

Specifically, comparisons were made when the length of the wound and angle of the spiral vessel in the axial direction were varied. The experimental apparatus shown in Fig. 7 was used for comparison. The regulator was changed to an electropneumatic regulator, and the flowmeter was changed to a more accurate one with a minimum sensitivity of 0.01 L/min using the test apparatus shown in Fig. 19. The pressure applied to the membrane was increased using an electropneumatic regulator. Consequently, the pressure at which air leakage occurred was recorded as the pressure limit and compared to evaluate the quantitative self-healing capability of the devised mechanism.

### C. 4.4 Assessment of wound length and self-repair capacity

First, the wound length and its self-repairing ability were evaluated. Three types of wounds were compared: 10, 15, and 20 mm perpendicular to the helix axis. The amount of material poured into the wound during the self-repair was 2 mL each. For each of the three conditions, three individuals were prepared, and the process from damage to self-repair and measurement of the pressure-resistance limit were performed.

Fig. 20 shows the experimental results for the individuals that withstood the highest pressure under each condition. The

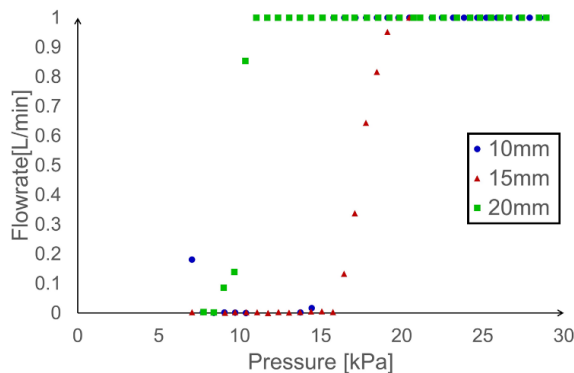


Figure 20. Result of the pressure test when the length of the wound is changed.

TABLE III. PRESSURE AT RE-LEAKAGE OCCURRING AFTER SELF-HEALING

	Sample 1	Sample 2	Sample 3
10 mm	14.8 kPa	10.5 kPa	6.8 kPa
15 mm	9.1 kPa	16.5 kPa	10.5 kPa
20 mm	9.1 kPa	6.8 kPa	6.8 kPa

convergence value of the flow rate at each step is shown in Fig. 20. When the flow rate converged to 0 L/min, no air leakage occurred at that pressure. Therefore, from the graph in Fig. 20, it can be read that no air leakage occurred up to 14.8 kPa at 10 mm, 16.5 kPa at 15 mm, and 9.1 kPa at 20 mm.

The results of these experiments are summarized in Table 3. The experimental results show that the pressure resistance at 15 mm was the highest among the three conditions; however, the difference from 10 mm was minimal and considered to be within the range of individual differences. Moreover, the pressure resistance limit of 20 mm was lower than that of the other two conditions, suggesting that the effect of self-healing was smaller. This may be attributed to the fact that the liquid material did not fully penetrate to the edge of the wound in the case of a large wound. From the above results, the self-healing ability decreased for larger wounds, with a peak between 15–20 mm.

### D. Assessment of wound angles and self-repair capacity

Scratch angles and self-healing abilities were evaluated. The self-healing conditions were the same as those described in the previous section. The length of the wound was maintained at 15 mm, and the conditions were set in 45° increments with respect to the helical axis and perpendicular direction. The experiments were conducted on three individuals under each condition, and the pressure resistance limits were measured.

Fig. 21 shows the convergence value of the flow rate at each step for the individual with the highest withstanding pressure limit under each condition. Table 4 summarizes the pressure resistance limits for each individual. The maximum values were the highest for the 90° case, that is, the axial helix wound, followed by the 135°, 45°, and 0° cases. The 135° case withstood pressures higher than 45° and 135°; however, the difference was small. This is because the helix is more vulnerable to damage as it approaches the axial direction. This is attributed to the fact that the liquid material flowed into the entire wound more easily as the flow path area in the wound cross section became larger when the axial direction was approached.

### E. Summary of evaluation experiments

The experiments confirmed that self-repair could not completely close the wound in the case of large wounds. In addition, self-repair did not function well under the other experimental conditions, and air leakage remained in certain cases. This may be attributed to the excessive contraction during pressure release, which caused the wound cross section to face downward, thereby allowing more liquid material to flow onto the bottom surface, which does not have a water-absorbent surface. However, even when the self-healing failed, the pressure resistance capacity was improved by pouring the

liquid material again. This is because the gel formed by the first pouring prevented the liquid material from flowing to areas other than the wound during the second pouring. Fig. 22 shows the self-repair of the robotic vascular mechanism with a fabric that has a liquid-absorbing function on its surface as well as its ability to expand after self-repair without causing air leakage when internal pressure is applied.

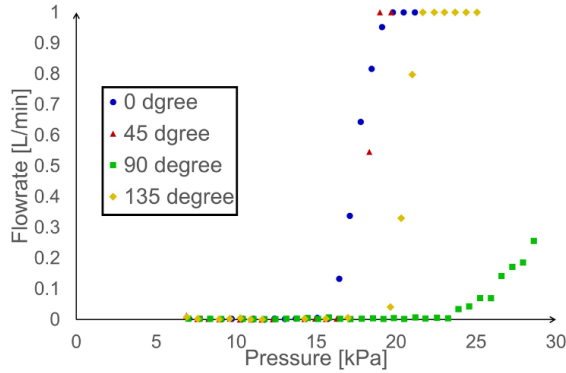


Figure 21. Result of the pressure test when the angle of the wound is changed.

TABLE IV. PRESSURE AT RE-LEAKAGE OCCURRING AFTER SELF-HEALING

	Sample 1	Sample 2	Sample 3
<b>0 deg</b>	9.1 kPa	16.5 kPa	10.5 kPa
<b>45 deg</b>	6.8 kPa	11.0 kPa	18.4 kPa
<b>90 deg</b>	6.8 kPa	24.0 kPa	15.8 kPa
<b>135 deg</b>	8.4 kPa	13.0 kPa	19.7 kPa

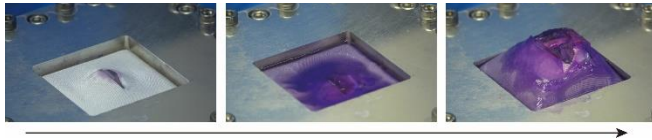


Figure 22. Self-Healing Process of the Robotic Blood Vessel Mechanism and Expanding motion after healing

## VI. CONCLUSION AND FUTURE ISSUES

This study proposed and realized a robotic vascular mechanism that actively repairs itself by sealing wound-like blood in a living body. Consequently, we confirmed that the self-repair capability can be improved by placing a water-absorbent material on the surface. Furthermore, we quantitatively evaluated the self-repair capability of the designed mechanism by comparing its pressure resistance when the length and angle of the wound were varied. The experimental results confirmed that the self-healing capability improved as the channel area in the wound cross-section increased.

In the future, we will consider the placement of water-absorbent materials on both sides of the membrane because there have been cases of liquid material leaking out of the

lower part of the membrane. In addition, although this study discusses a one-time injury, we will investigate a vascular structure that can function as a self-repair system even in the case of a second injury.

## REFERENCES

- [1] S. Terryn, J. Brancart, V.A. Assche, and B Vanderborght, "Self-healing soft pneumatic robots," *Sci. Robot.*, vol. 2, no. 9, 2017.
- [2] S. R. White, N. R. Sottos, P. H. Geubelle, J. S. Moore, M. R. Kessler, S. R. Sriram, E. N. Brown, and S. Viswanathan, "Autonomic healing of polymer composites," *Nature*, vol. 409, pp. 794, 2001.
- [3] X. Chen, M. A. Dam, K. Ono, A. Mal, H. Shen, S. R. Nutt, K. Sheran, and F. Wudl, "A thermally re-mendable cross-linked polymeric material," *Science*, vol. 295, no. 5560, pp. 1698–1702, 2002.
- [4] M. Nakahata, Y. Takahashi, and A. Harada, "Highly Flexible, Tough, and Self-Healing Supramolecular Polymeric Materials Using Host - Guest Interaction," *Macromol. Rapid Commun.*, vol. 37, no. 1, pp. 86–92, 2015.
- [5] K. Nagaya, S. Ibiraki, M. Chiba, and K. Cho, "Development of Tires that Repair Themselves after Holes," *Trans. Jap. Soc. Mech. Eng. (C)*, vol. 71, no. 708, pp. 2635–2642, 2005.
- [6] S. Inomata, T. Iijima, Y. Yamazaki, I. Onda, T. Takahashi, M. Watanabe, K. Tadakuma, H. Furukawa, M. Konyo, and S. Tadokoro, "Soft robot vascular mechanism for self-repair function," *The Proceedings of JSME annual Conference on Robotics and Mechatronics 2020*, 1P 2-J16, 2020.
- [7] S. Inomata, Y. Yamazaki, I. Shiga, M. Kameoka, S. M. N. Islam, M. Watanabe, E. Takane, K. Tadakuma, H. Furukawa, M. Konyo, S. Tadokoro, "Active self-healing soft robotic vascular mechanism," *38th Annual Conference of the Robotic Society of Japan*, 1, A1-03, 2020.
- [8] J. Saito, H. Furukawa, T. Kurokawa, N. Kuwabara, S. Kuroda, J. Hu, Y. Tanaka, J. P. Gong, N. Kitamura, and K. Yasuda, "Robust bonding and one-step facile synthesis of tough hydrogels with desirable shape by virtue of the double network structure," *Polym. Chem.*, vol. 2, no. 3, pp. 575–580, 2011.
- [9] Press Release, "Development of Flexible Robot Hand that Can Grasp Even Pointy Objects Like Blades – Realization of High Cut Resistance and Durability that Does Not Break Even in Rubble," Tohoku University, International Rescue System Research Institute, Japan Science and Technology Agency (JST), Director-General for Policy Management (Science, Technology, and Innovation), Cabinet Office, 14th June 2018.
- [10] Y. Takahashi, E. Takane, M. Watanabe, K. Tadakuma, M. Konyo, and S. Tadokoro, "Secondary Moment Type Flexural Switching Mechanism with Cross Section," *The 21st SICE Conference on System Integration*, 2E3-04, pp. 1841–1846, Fukuoka (online meeting), December 16–18, 2020.
- [11] S. R. WHITE, J. S. MOORE, N. R. SOTTOS, B. P. KRULL, W. A. SANTA CRUZ, AND R. C. R. "Restoration of Large Damage Volumes in Polymers," *SCIENCE*, 9 May 2014, Vol 344, Issue 6184, pp. 620–623, DOI: 10.1126/science.1251113
- [12] Md. Ariful Islam, Labanya Talukder, Md. Firoj Al, Subrata K. Sarker, S. M. Mueen, Prangon Das, Md. Mehedi Hasan, Sajal K. Das, Md. Manirul Islam, Md. Robiul Islam, Sumaya Ishrat Moyeen, Faisal R. Badal, Md. Hafiz Ahamed, Sarafat Hussain Abhi, "A review on self-healing featured soft robotics," *REVIEW article*, *Front. Robot. AI*, 26 October 2023, Sec. Soft Robotics, Volume 10 - 2023 | <https://doi.org/10.3389/frobot.2023.1202584>
- [13] Seppe Terryn, Jakob Langenbach, Ellen Roels, Joost Brancart, Camille Bakkali-Hassani, Quentin-Arthur Poutrel, Antonia Georgopoulou, Thomas George Thuruthel, Ali Safaei, Pasquale Ferrentino, Tutu Sebastian, Sophie Norvez, Fumiya Iida, Anton W. Bosman, François Tournilhac, Frank Clemens, Guy Van Assche, Bram Vanderborght, "A review on self-healing polymers for soft robotics," *Materials Today*, Volume 47, July–August 2021, Pages 187–205.
- [14] Tadakuma, K., Kawakami, M. and Furukawa, H., 2022. From a Deployable Soft Mechanism Inspired by a Nemertea Proboscis to a Robotic Blood Vessel Mechanism. *Journal of Robotics and Mechatronics*, 34(2), pp.234–239.